# Leak detection in virtually isolated pipe sections within a complex pipe system using a two-source-four-sensor transient testing configuration

He Shi, Jinzhe Gong, Angus R. Simpson, Aaron C. Zecchin and Martin F. Lambert

## ABSTRACT

Leak detection in complex pipeline systems is challenging due to complex wave reflections. This research proposes a new technique for leak detection in targeted pipe sections within complex water supply pipe systems using controlled hydraulic transient pressure waves. To 'virtually isolate' a targeted pipe section for independent analysis, a two-source-four-sensor transient testing configuration is used to extract the transfer matrix of the targeted pipe section, and it is independent of the system boundary conditions. The imaginary part of the difference between two elements in the transfer matrix is sensitive to leaks. The result should be zero if no leak is present, while a leak will introduce a sinusoidal pattern. An algorithm is developed to extract the leak information, which is applicable to multiple leaks. Two numerical case studies are conducted to validate the new leak detection technique. Case 1 is on a single pipe system with two leaks and deteriorated pipe sections, and pulse pressure waves are used as the excitation. Case 2 is on a simple pipe network with one leak, and pseudo-random binary signals are used as the excitation. The successful determination of the leak location and impedance validates the concept.

**Key words** | hydraulic transient, leak detection, transfer matrix, water distribution systems, water hammer

**He Shi**
**Angus R. Simpson**
**Aaron C. Zecchin**
**Martin F. Lambert**
School of Civil, Environmental and Mining Engineering,
University of Adelaide,
North Terrace, Adelaide, SA 5005,
Australia

**Jinzhe Gong** (corresponding author)
School of Engineering,
Deakin University,
75 Pigdons Rd, Waurn Ponds, VIC 3216,
Australia
E-mail: *james.gong@deakin.edu.au*

## INTRODUCTION

Leakage in water distribution systems (WDSs) is a global issue, and the leakage rate ranges from about 10% in well-maintained WDSs (Beuken *et al.* 2006) to above 50% in poorly managed systems (Mutikanga *et al.* 2009). Leak detection in WDSs, however, is challenging due to the sheer size of the pipe network and the fact that most pipes are buried under ground.

Acoustic correlation analysis is the most commonly used technique for leak detection in water pipelines (Li *et al.* 2015). Two acoustic sensors are attached to two separate fittings on a pipeline and record vibrations on the fitting (using accelerometers) or the acoustic pressure in water (using hydrophones). The acoustic correlation-based leak detection techniques are relatively easy to implement since only passive listening is required. However, the weak leak-induced acoustic waves can only propagate limited distances (Butterfield *et al.* 2018).

An alternative is the hydraulic transient-based leak detection approach (Puust *et al.* 2010). Controlled hydraulic transient pressure waves can be generated in pipelines by transient wave generators. Usable devices include fast-acting solenoid valves (Shucksmith *et al.* 2012; Gong *et al.* 2016a), portable pressure tanks (Brunone *et al.* 2008), and spark plugs (Gong *et al.* 2018a). The incident wave typically has a magnitude of a few meters of pressure head and propagates along the pipe under test at high speed (around 1,200 m/s in metallic pipes). Wave reflections occur at physical discontinuities (e.g. a leak) and can be measured by

doi: 10.2166/hydro.2020.170

pressure transducers. Over the past two decades, a number of transient-based leak detection techniques have been developed, and they can be generally allocated into the following categories: (1) techniques that analyze wave reflections (either from the raw data or pre-processed data) using principles of time domain reflectometry (TDR) (Shucksmith *et al.* 2012; Meniconi *et al.* 2015; Nguyen *et al.* 2018); (2) techniques that analyze the frequency response function (FRF) of a pipe system (Covas *et al.* 2005; Lee *et al.* 2005; Gong *et al.* 2013b; Duan 2016); (3) techniques that focus on the damping of transient pressure responses in a pipeline system (Wang *et al.* 2002; Brunone *et al.* 2018); (4) inverse transient analysis (ITA)-based techniques that search for an optimal numerical pipe model whose response matches the pressure measurements (Soares *et al.* 2010; Capponi *et al.* 2017); and (5) new techniques involving advanced mathematical analysis and signal processing (Cugueró-Escofet *et al.* 2016; Wang *et al.* 2019). The transient-based techniques are attractive because a single test can cover up to kilometers of pipe length (Meniconi *et al.* 2011; Gong *et al.* 2015), and the active testing approach can reveal other information such as blockages (Meniconi *et al.* 2013) and pipe wall condition (Gong *et al.* 2016b; Zhang *et al.* 2018; Shi *et al.* 2019).

Despite the fact that many transient-based leak detection techniques have been proposed, applications in real water pipeline systems are limited. A significant challenge to all the transient-based techniques is the complexity of real water pipeline systems. For the TDR-based techniques, leak-induced reflections can be difficult to distinguish from other reflections, such as those from cross-connections and unknown wall thickness changes. The FRF of a single pipe system is more sensitive to leaks than extended wall thickness changes (Duan *et al.* 2011a); therefore, the FRF-based techniques are advantageous over the TDR-based techniques in detecting small leaks. However, most FRF-based techniques are only applicable to reservoir–pipeline–reservoir (R–P–R) or reservoir–pipeline–valve (R–P–V) systems. Duan (2016) has recently extended the FRF-based leak detection to simple pipe systems with a branch or a loop. The conventional FRF-based approach is difficult to be further extended to more complex pipe systems, because the FRF considered in all previous studies is a representation of the overall system, and complex systems will produce FRFs that are too complex to analyze.

The current research proposes a new frequency–domain technique for leak detection in targeted pipe sections. A key innovation of the new technique is the concept of utilizing a special transient pressure generation and sensing configuration, combined with custom-developed signal processing algorithms, to virtually break any complex pipeline systems down to its simplest form – a single pipe section – for independent condition diagnosis. The proposed approach is opposite to the conventional research idea of gradually adapting the transient-based leak detection techniques developed for simple pipeline systems (e.g. R–P–R or R–P–V systems) to more complex pipe networks (Ghazali *et al.* 2012; Duan 2016; Capponi *et al.* 2017).

The virtual isolation of a pipe section is achieved by a two-source-four-sensor transient testing strategy, which enables the extraction of the transfer matrix (Wylie & Streeter 1993; Chaudhry 2014) of a selected pipe section out of any complex pipe system. This testing strategy was originally developed and used in the field of acoustic analysis of ducts (Munjal & Doige 1990; Salissou & Panneton 2010), and recently, it was validated using a short water pipeline in the laboratory by Yamamoto *et al.* (2015) for studying the transfer matrix of resistance (orifices) and compliance (trapped air). Note that the focus of Yamamoto *et al.* (2015) was purely on the individual components, and not on long pipe sub-systems. The current research adapts this technique to the transfer matrix extraction of long sections in complex water pipe systems, with significantly more complex wave interaction phenomena.

A major contribution of the current research is the development of a new leak detection algorithm based on the analysis of the transfer matrix of a virtually isolated pipe section. This transfer matrix is related to the virtually isolated pipe section only and is independent from any complexities of the rest of the pipe system (e.g. boundary conditions or other network connectivity). As a result, the extracted transfer matrix is much simpler than the transfer matrix of the overall pipe system, and the analysis is more straightforward than conventional FRF-based techniques. The proposed new algorithm can determine the number of leaks as well as their locations and impedance (which relates to the size of the leak).

In the following, the technique for extracting the transfer matrix of a targeted pipe section and the new algorithm for leak detection of a virtually isolated pipe section are described. Two numerical case studies (a simple pipeline system and a simple pipe network) are conducted to validate the transfer matrix extraction technique and the proposed leak detection algorithm. A sensitivity analysis to leak size and measurement noise is conducted. Challenges in real world applications are also discussed.

## TRANSFER MATRIX EXTRACTION FOR A TARGETED PIPE SECTION

### Transfer matrix of a uniform pipe section

For a uniform single pipe section, the relation between the two sets of pressure and flow as observed at the two ends of the section can be written as (Wylie & Streeter 1993; Chaudhry 2014)

$$\begin{Bmatrix} Q \\ H \end{Bmatrix}_{\mathrm{D}} = \begin{bmatrix} \cos h(\mu L) & -\frac{1}{Z_{\mathrm{P}}}\sin h(\mu L) \\ -Z_{\mathrm{P}}\sin h(\mu L) & \cos h(\mu L) \end{bmatrix} \begin{Bmatrix} Q \\ H \end{Bmatrix}_{\mathrm{U}} \tag{1}$$

where $H$ and $Q$ are complex pressure head and flow in the frequency domain; the footnotes 'D' and 'U' represent the downstream and the upstream boundary of the pipe section, respectively; $L$ is the length of the pipe; $Z_{\mathrm{P}}$ is the characteristic impedance of the pipe section; and $\mu$ is the propagation factor.

The propagation factor is described by (Wylie & Streeter 1993; Chaudhry 2014)

$$\mu = \frac{\sqrt{-\omega^2 + j\omega g A R}}{a} \tag{2}$$

where $\omega$ is the angular frequency; $j = \sqrt{-1}$ is the imaginary unit; $g$ is the gravitational acceleration; $A$ is the cross-sectional area of the pipe; $a$ is the wave speed; and $R$ is the frictional resistance term. For turbulent and laminar flows, $R = fQ_0/(gDA^2)$ and $R = 32\nu/(gD^2A)$, respectively, in which $f$ is the Darcy–Weisbach friction factor; $Q_0$ is the steady-state flow rate; $D$ is the diameter of the pipe; and $\nu$ is the kinematic viscosity of the fluid.

The characteristic impedance is (Wylie & Streeter 1993; Chaudhry 2014)

$$Z_{\mathrm{P}} = \frac{\mu a^2}{j\omega g A} \tag{3}$$

### Two-source-four-sensor testing strategy for water pipes

The proposed configuration for extracting the transfer matrix of a targeted pipeline section using the two-source-four-sensor strategy and hydraulic transient testing is illustrated in Figure 1. Two pairs of pressure transducers ($T_A$, $T_B$ and $T_C$, $T_D$) bracket the section of pipe under investigation. The distance between the two transducers in each pair, $L_{AB}$, for the distance between $T_A$ and $T_B$, and $L_{CD}$ for that between $T_C$ and $T_D$, is recommended to be short (recommended to be 2 m or less) in real pipelines, such that the transfer function of the short pipe reach can be calibrated or theoretically determined (Shi *et al.* 2017). Two

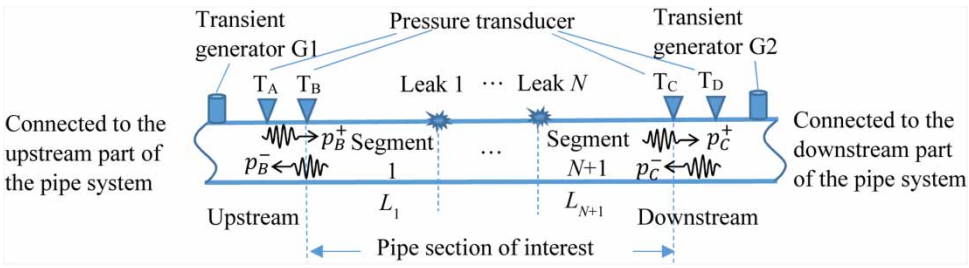


**Figure 1** | Test configuration for extracting the transfer matrix of a targeted pipe section with $N$ leaks.

transient pressure wave generators are installed, with one on each side of the pipe section of interest, and they will be used in sequence.

The pipe section between transducers $T_B$ and $T_C$ can be considered as a linear time-invariant (LTI) system. The directional travelling waves $p_B^+$ and $p_C^-$ which are travelling into the pipe section are considered as the input to the LTI system, while the waves $p_B^-$ and $p_C^+$ that are travelling out of the section are taken as the output. A pair of directional travelling pressure waves (e.g. $p_B^+$ and $p_B^-$) can be determined from the pressure waves (pressure perturbations) measured by each of the two pairs of transducers (e.g. $p_A$ and $p_B$ as the pressure perturbations measured by $T_A$ and $T_B$) using a wave separation technique (Shi *et al.* 2017). Once the directional pressure waves at both boundaries of a pipe section are obtained, the pipe section can be regarded as an independent system since the boundary conditions are entirely specified. As a result, two pairs of transducers enable the analysis of a specific section of pipe independently from the complexities of the rest of the pipeline system (therefore considered as 'virtually isolated').

## Determination of the transfer matrix using pressure measurements

For a pipe section with unknown conditions, the transfer matrix have four elements ($U_{11}$, $U_{12}$, $U_{21}$, and $U_{22}$) to be determined. Two independent transient tests are needed to establish four equations to solve these four unknowns. This is achieved by generating transient excitation from the two sides of the pipe section one at a time and measures the pressure responses by the four transducers in each test. Wide-based transient signals are preferred, but the signals generated on the two sides by the two generators do not have to be identical. Based on Equation (1), the flowing matrix can be established:

$$\begin{bmatrix} Q_{C1} & Q_{C2} \\ H_{C1} & H_{C2} \end{bmatrix} = \begin{bmatrix} U_{11} & U_{12} \\ U_{21} & U_{22} \end{bmatrix} \begin{bmatrix} Q_{B1} & Q_{B2} \\ H_{B1} & H_{B2} \end{bmatrix} \tag{4}$$

where $H_{B1}$, $Q_{B1}$, $H_{C1}$, and $Q_{C1}$ are the complex pressure head and flow in the first transient test (using transient generator 1), and $H_{B2}$, $Q_{B2}$, $H_{C2}$, and $Q_{C2}$ are the parameters in the second test (using transient generator 2). The complex head parameters at the location of $T_B$ ($H_{B1}$ and $H_{B2}$) and those at the location of $T_C$ ($H_{C1}$ and $H_{C2}$) can be readily obtained by transforming the measured time domain pressure perturbations ($p_B$ and $p_C$) into the frequency domain. The complex flow parameters ($Q_{B1}$, $Q_{B2}$, $Q_{C1}$, and $Q_{C2}$) are not directly measured but can be obtained from the directional pressure waves (Yamamoto *et al.* 2015).

The directional pressure waves (as in the frequency domain) at the location of $T_B$, for example, can be described by (Shi *et al.* 2017)

$$P_B^+ = \frac{P_A S_{AB} - P_B S_{AB}^2}{1 - S_{AB}^2} \tag{5}$$

$$P_B^- = \frac{P_B - P_A S_{AB}}{1 - S_{AB}^2} \tag{6}$$

where capital $P$ is used to represent pressure waves in the frequency domain and to differentiate from the time domain counterparts denoted in early sections using lower case $p$; $S_{AB}$ is the transfer function of the short pipe section between $T_A$ and $T_B$, and its expression is

$$S_{AB}(i\omega) = e^{-\mu L_{AB}} \tag{7}$$

The complex flow can be calculated by (Yamamoto *et al.* 2015)

$$Q_B = \frac{P_B^+ - P_B^-}{Z_P} \tag{8}$$

As a result, the complex flow $Q$ can be determined from the pressure measurements, the transfer function of the short pipe reach between the two pressure transducers, and the characteristic impedance of the pipeline, and the expression for $Q_B$ is

$$Q_B = \frac{2P_A S_{AB} - P_B - P_B S_{AB}^2}{Z_P(1 - S_{AB}^2)} \tag{9}$$

Once the head and flow are all known, elements in the transfer matrix can be obtained by solving the matrix in Equation (4).

## LEAK DETECTION FOR A TARGETED PIPE SECTION USING THE TRANSFER MATRIX

Existing FRF-based leak detection techniques have to consider the pipe boundary conditions (typically a valve or a reservoir). In contrast, the proposed new technique in this research is independent from the boundary conditions of a pipe system due to the 'virtual isolation' using the two-source-four-sensor strategy. As a result, the following derivation considers a single pipeline section only (with leaks but no boundary elements), and this is different from the existing research.

### Transfer matrix for a pipe section with leaks

For a uniform pipe section with $N$ leaks, as depicted in Figure 1, the relationship between the two sets of pressure and flow as observed at the two boundaries can be written as

$$\begin{Bmatrix} Q \\ H \end{Bmatrix}_{\mathrm{D}} = \mathbf{U}_N \begin{Bmatrix} Q \\ H \end{Bmatrix}_{\mathrm{U}} \tag{10}$$

where $\mathbf{U}_N$ is the overall transfer matrix for the pipe section with $N$ leaks. Considering the effect of pipe wall friction is small for large diameter water pipelines and to highlight the leak-induced effect, the effect of friction is neglected in the following derivation but discussed later. The field matrix $\mathbf{F_i}$ for a frictionless and uniform pipe segment $i$ is given as (Chaudhry 2014)

$$\mathbf{F_i} = \begin{bmatrix} \cos\left(\frac{\omega L_i}{a}\right) & -\frac{j}{Z_c}\sin\left(\frac{\omega L_i}{a}\right) \\ -jZ_c\sin\left(\frac{\omega L_i}{a}\right) & \cos\left(\frac{\omega L_i}{a}\right) \end{bmatrix} \tag{11}$$

where $Z_c = a/gA$, and it is the characteristic impedance of the frictionless pipe; and $L_i$ is the length of the $i$th pipe segment.

The point matrix $\mathbf{P}_i$ for the $i$th leak is given as (Lee *et al.* 2005; Gong *et al.* 2013b)

$$\mathbf{P}_i = \begin{bmatrix} 1 & -\frac{1}{Z_{Li}} \\ 0 & 1 \end{bmatrix} \tag{12}$$

where $Z_{Li} = 2H_{Li}/Q_{Li}$, and it is the impedance of the $i$th leak, $H_{Li}$ is the steady-state head at the leak and $Q_{Li}$ is the steady-state discharge out of the leak.

The overall transfer matrix $\mathbf{U}_N$ for the pipe section with $N$ leaks can be expressed by multiplying the field matrices and point matrices from downstream to upstream and written as

$$\mathbf{U}_N = \begin{bmatrix} U_{11.N} & U_{12.N} \\ U_{21.N} & U_{22.N} \end{bmatrix} = \mathbf{F}_{N+1}\mathbf{P}_N \ldots \mathbf{F_2}\mathbf{P}_1\mathbf{F}_1 \tag{13}$$

where the footnote $N$ denotes the number of leaks in the pipe section.

Now considering a uniform pipe section with one leak, the overall transfer matrix $\mathbf{U}_1$ is

$$\mathbf{U}_1 = \begin{bmatrix} U_{11.1} & U_{12.1} \\ U_{21.1} & U_{22.1} \end{bmatrix} = \mathbf{F_2}\mathbf{P}_1\mathbf{F}_1 \tag{14}$$

After substituting Equations (11) and (12) into Equation (14) and performing appropriate matrix operations, the analytical expressions of the transfer matrix elements are given as

$$U_{11.1} = \cos\left(\frac{\omega L}{a}\right) + \frac{jZ_c}{2Z_{L1}}\sin\left(\frac{\omega L}{a}\right) - \frac{jZ_c}{2Z_{L1}}\sin\left[\frac{(1-2x_{L1})\omega L}{a}\right] \tag{15}$$

$$U_{12.1} = -\frac{j}{Z_c}\sin\left(\frac{\omega L}{a}\right) - \frac{1}{2Z_{L1}}\cos\left(\frac{\omega L}{a}\right) - \frac{1}{2Z_{L1}}\cos\left[\frac{(1-2x_{L1})\omega L}{a}\right] \tag{16}$$

$$U_{21.1} = -jZ_c\sin\left(\frac{\omega L}{a}\right) - \frac{Z_c^2}{2Z_{L1}}\cos\left(\frac{\omega L}{a}\right) + \frac{Z_c^2}{2Z_{L1}}\cos\left[\frac{(1-2x_{L1})\omega L}{a}\right] \tag{17}$$

$$U_{22.1} = \cos\left(\frac{\omega L}{a}\right) + \frac{jZ_c}{2Z_{L1}}\sin\left(\frac{\omega L}{a}\right) + \frac{jZ_c}{2Z_{L1}}\sin\left[\frac{(1-2x_{L1})\omega L}{a}\right] \tag{18}$$

where $x_{L1}$ is the dimensionless leak location, which is defined as the ratio of the distance from the leak to the upstream end of the pipe to the total length of the pipe $L$.

For the $i$th leak, $x_{Li} = (L_1 + L_2 + \ldots + L_i)/L$. The transfer matrix $\mathbf{U}_N$ for a pipe section with $N$ leaks can be derived following the same procedure.

## Extraction of the leak-induced feature

The impact of a leak on the transfer matrix can be seen through comparing the transfer matrix of the pipe section with one leak [Equations (15)–(18)] with that of an intact pipe [Equation (11)]. In this research, a new discovery is that the imaginary part of $U_{22} - U_{11}$ is sensitive to the leak location and size. When there is no leak, $U_{22} - U_{11}$ is null since the two elements should be identical according to Equations (1) and (11).

For a pipe section with only one leak, the imaginary part of the difference between $U_{22.1}$ [Equation (18)] and $U_{11.1}$ [Equation (15)] is defined as $T_1$ and given as

$$T_1 = \mathrm{Im}\{U_{22.1} - U_{11.1}\} = \frac{Z_c}{Z_{L1}} \sin\left[\frac{(1-2x_{L1})L\omega}{a}\right] \tag{19}$$

where Im{ } gives the imaginary part of the parameter in the bracket.

It can be seen from Equation (19) that $T_1$ is a sinusoidal function that is related to the leak impedance (which relates to the leak size) and the leak location (except for a leak at a normalized location of 0.5). The leak locations define the period of the sinusoidal pattern and the leak impedance defines the amplitude of the pattern. This finding is similar to that observed from the pressure response of a reservoir–pipeline–valve (R–P–V) system with a leak (Lee *et al.* 2005); however, this sinusoidal function is different from the one observed in the previous work. The expression in Equation (19) is much simpler and independent from any boundary conditions.

Using the same approach as outlined above, the leak-induced effects for a pipe system with two leaks, $T_2$, can be derived as

$$T_2 = \mathrm{Im}\{U_{22.2} - U_{11.2}\} = \frac{Z_c}{Z_{L1}} \sin\left[\frac{(1-2x_{L1})L\omega}{a}\right] + \frac{Z_c}{Z_{L2}} \sin\left[\frac{(1-2x_{L2})L\omega}{a}\right] \tag{20}$$

Equation (20) indicates that two leaks will introduce two sinusoidal patterns with different periods.

For a pipe system with three leaks, the analytical expression of $T_3$ is derived as

$$T_3 = \mathrm{Im}\{U_{22.3} - U_{11.3}\} = \frac{Z_c}{Z_{L1}} \sin\left[\frac{(1-2x_{L1})L\omega}{a}\right] + \frac{Z_c}{Z_{L2}} \sin\left[\frac{(1-2x_{L2})L\omega}{a}\right] + \frac{Z_c}{Z_{L3}} \sin\left[\frac{(1-2x_{L3})L\omega}{a}\right] + T_h \tag{21}$$

where $T_h$ is a higher-order term

$$T_h = \frac{Z_c Z_c Z_c}{4 Z_{L1} Z_{L2} Z_{L3}} \left\{ \begin{array}{l} \sin[(1-2x_{L1})L\omega/a] - \\ \sin[(1-2x_{L2})L\omega/a] + \\ \sin[(1-2x_{L3})L\omega/a] + \\ \sin[(1-2x_{L1}+2x_{L2}-2x_{L3})L\omega/a] \end{array} \right\} \tag{22}$$

The ratio of the characteristic impedance of pipe and the impedance of the $i$th leak can be described as

$$\frac{Z_c}{Z_{Li}} = \frac{a}{\sqrt{2gH_L}} \frac{C_d A_L}{A} \tag{23}$$

where $C_d A_L/A$ is the normalized leak size. For small leaks (which are difficult to detect by conventional techniques and are the focus of this research), the impedance of the leak is much larger than the characteristic impedance of the pipe (i.e. the value of $Z_c/Z_{Li}$ is much smaller than 1). Consequently, the value of the higher-order term $T_h$ will be significantly smaller than the values of the first three items in Equation (21) and negligible. For a pipe section with more than three leaks, the higher-order term will be even smaller. As a result, the leak-induced effect on the transfer matrix of a pipe section with $N$ leaks can be described as

$$T_N = \mathrm{Im}\{U_{22.N} - U_{11.N}\} = \sum_{i=1}^{N} \frac{Z_c}{Z_{Li}} \sin\left[\frac{(1-2x_{Li})L\omega}{a}\right] \tag{24}$$

## Determination of the leak location and size

$T_N$ in Equation (24) is a frequency domain signal with the $x$-axis being the frequency and in the unit of Hz. If we

assume the $x$-axis to be a time axis, the leak-induced signal $T_N$ has a wave form equivalent to a superposition of $N$ sinusoidal waves. The period/frequency of each sinusoidal wave corresponds to the location of a leak, and the amplitude is related to the leak impedance. In other words, the frequency and amplitude of each sinusoidal wave in the $T_N$ signal can be used to determine the location and impedance (size) of a leak.

The frequency and amplitude information of the $N$ sinusoidal waves can be extracted by applying the Fourier transform to the $T_N$ signal (i.e. treat it like a time domain signal) and analyzing the resultant signal $T_N^*$. Since the leak-induced signals in $T_N$ are sinusoidal waves, based on the theory of the discrete Fourier transform (Oppenheim *et al.* 1997), each leak will be represented by a spike in the imaginary part of $T_N^*$. If the normalized leak location is in the range of (0, 0.5), the corresponding spike in the imaginary part of $T_N^*$ will be negative in value; if the normalized leak location is in the range of (0.5, 1), the corresponding spike will be positive in value. As a result, the location of the $i$th leak is determined by

$$x_{Li} = \frac{1}{2} + \mathrm{Sgn}\{\mathrm{Im}\{T_N^*(F_{Pi})\}\}\left(\frac{F_{Pi}a}{2L}\right) \tag{25}$$

where $F_{Pi}$ is the 'frequency' that corresponds to the $i$th peak in the imaginary part of $T_N^*$, $T_N^*(F_{Pi})$ is the complex value at the peak frequency, and Sgn{ } assesses the sign of the parameter in the bracket.

The ratio of the pipe characteristic impedance to the impedance of the $i$th leak is determined by

$$\frac{Z_c}{Z_{Li}} = 2\mathrm{Abs}\{T_N^*(F_{Pi})\} \tag{26}$$

where Abs { } gives the absolute value of the parameter in the bracket. The effective leak size can be determined by substituting Equation (26) into Equation (23) and performing appropriate mathematical operations, with the final expression being

$$C_d A_L = 2\mathrm{Abs}\{T_N^*(F_{Pi})\}\frac{A\sqrt{2gH_L}}{a} \tag{27}$$

## NUMERICAL SIMULATIONS

Two numerical case studies are conducted to validate the proposed targeted leak detection technique. The system in Case 1 is a transmission main and that in Case 2 is a water distribution network.

### Case 1: A single pipe with two leaks

#### System information

The layout of the pipeline system studied in Case 1 is given in Figure 2. The system is an R–P–V system with two leaks and two deteriorated pipe sections (e.g. sections with extended corrosion). The pipe deterioration is represented by a reduction in wave speed. The pipe section of interest (the targeted pipe section) is the section between $T_B$ and $T_C$. The length information is given in Figure 2, and other system parameters are summarized in Table 1. The normalized leak locations are $x_{L1} = 0.2$ and $x_{L2} = 0.7$, respectively. The diameters of the two leaks are $D_{L1} = 6.8$ mm and $D_{L2} = 11.6$ mm. The relative leak sizes (effective leak

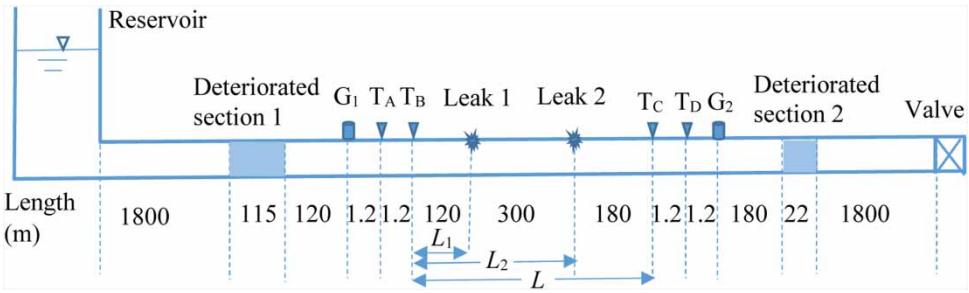


**Figure 2** | Layout of the single pipeline system in Case 1.

**Table 1** | System information for Case 1

| Parameter | Value |
|---|---|
| Reservoir head, $H_r$ | 60 m |
| Pipe internal diameter, $D$ | 500 mm |
| Diameter of Leak 1, $D_{L1}$ | 6.8 mm |
| Diameter of Leak 2, $D_{L2}$ | 11.6 mm |
| Leak discharge coefficient, $C_d$ | 0.6 |
| Effective opening area of Leak 1, $C_{d1}A_{L1}$ | 22 mm$^2$ |
| Effective opening area of Leak 2, $C_{d2}A_{L2}$ | 63 mm$^2$ |
| Relative size of Leak 1, $C_dA_{L1}/A$ | $1.1\times10^{-4}$ |
| Relative size of Leak 2, $C_dA_{L2}/A$ | $3.2\times10^{-4}$ |
| Steady-state flow through valve, $Q_0$ | 0.2 m$^3$/s |
| Steady-state flow through Leak 1, $Q_{L1}$ | 0.75 L/s |
| Steady-state flow through Leak 2, $Q_{L1}$ | 2.08 L/s |
| Wave speed in intact pipe, $a_0$ | 1,200 m/s |
| Wave speed in deteriorated section 1, $a_1$ | 1,150 m/s |
| Wave speed in deteriorated section 2, $a_2$ | 1,100 m/s |
| Darcy–Weisbach friction factor, $f$ | 0.015 |
| Normalized location of Leak 1, $x_{L1}$ | 0.2 |
| Normalized location of Leak 2, $x_{L2}$ | 0.7 |
| Impedance ratio of pipe to Leak 1, $Z_c/Z_{L1}$ | 0.00415 |
| Impedance ratio of pipe to Leak 2, $Z_c/Z_{L2}$ | 0.0116 |

opening relative to the pipe cross-sectional area) are $C_dA_{L1}/A = 1.1\times10^{-4}$ (0.11‰) and $C_dA_{L2}/A = 3.2\times10^{-4}$ (0.32‰), respectively.

## Pressure response

The method of characteristics (MOCs) (Wylie & Streeter 1993; Chaudhry 2014) is used to simulate the transient response of the pipeline system. Steady friction is considered to evaluate its impact on the leak detection. The time step used is 0.0001 s. Two transient tests are simulated: in the first test, a pulse pressure wave with a duration of 10 ms and a peak size of about 6 m is generated at $G_1$ (by opening and then closing a side-discharge valve); and in the second test, a pulse pressure wave with the same characteristics is generated at $G_2$. The pressure traces at $T_A$ and $T_D$ as obtained from the first test are shown in Figure 3. The standing pressure at $T_D$ is lower than that at $T_A$ because of the effect of steady friction. The two large pulses in the $T_A$ and $T_D$ traces are the incident pulse wave, arriving at $T_A$ and

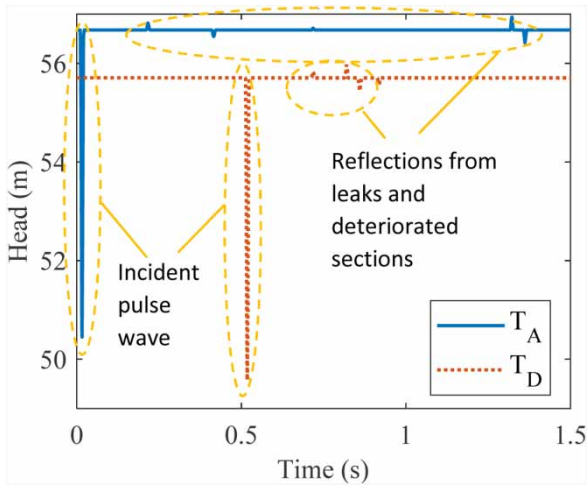


**Figure 3** | Pressure responses at $T_A$ and $T_D$ as obtained from transient test 1 (using generator G1) in Case 1.

$T_D$ in sequence. A number of small pulses can be seen in both traces, and they are reflections from the two leaks and the two deteriorated pipe sections. Due to the complexity introduced by the deteriorated pipe sections, it is difficult to identify the leaks from the pressure responses even if the reflections are clear.

## Transfer matrix extraction

The pressure measurements at $T_A$ to $T_D$ are transformed to the frequency domain by the Fourier transform after the steady-state head has been offset from the original measurement. The calculations outlined in previous sections are then conducted to obtain the transfer matrix for the pipe section between $T_B$ and $T_C$. The imaginary part of the numerically obtained transfer matrix element $U_{22}$ is shown in Figure 4, together with the theoretical counterpart for the same pipe section with two leaks and that for the same pipe section without any leak (only the results up to 30 Hz are shown for clarity). The theoretical results are calculated using Equation (13) with the friction effect neglected.

It can be seen from Figure 4 that the numerically determined Im{$U_{22}$} (solid line) is highly consistent with the theoretical result for the same pipe section with two leaks (dotted line), except for the small error close to the zero frequency. In contrast, the theoretical Im{$U_{22}$} for the same

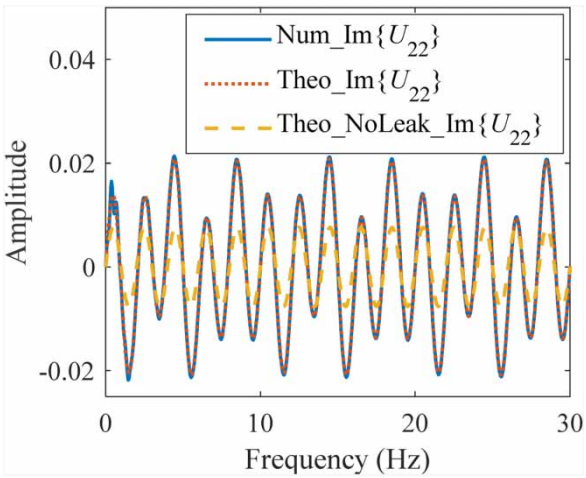


**Figure 4** | Imaginary part of transfer matrix element $U_{22}$ as obtained from numerical simulations and the transfer matrix extraction technique for the pipe section with two leaks in Case 1 (solid line), compared with the theoretical result for the same pipe section with two leaks (dotted line), and the theoretical result for the pipe section when it is intact (dashed line).

pipe section but with no leaks is quite different because it only has one sinusoidal component that is related to the fundamental frequency of the pipe section [refer to Equation (11)]. The results of $\mathrm{Im}\{U_{22} - U_{11}\}$ are then obtained from the numerically derived transfer matrix and also from analytical calculations [using Equation (20)], and the results are compared in Figure 5 (only the results up to 30 Hz are shown for clarity). The result obtained from the numerical simulations is highly consistent with the theoretical result.

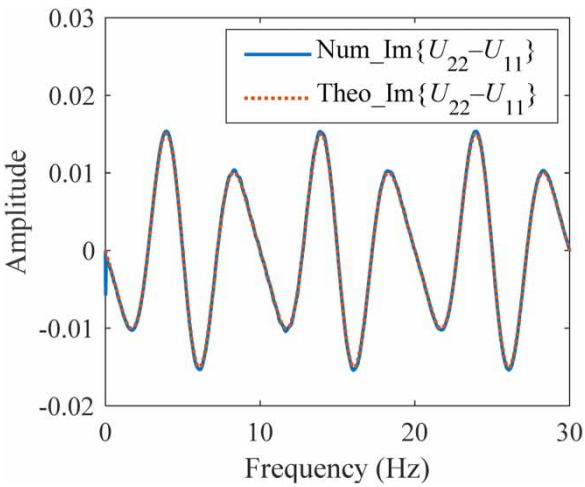


**Figure 5** | Imaginary part of ($U_{22} - U_{11}$) as obtained from numerical simulations and the transfer matrix extraction technique for the pipe section with two leaks in Case 1 (solid line), and the theoretical result for the same pipe section with two leaks (dotted line).

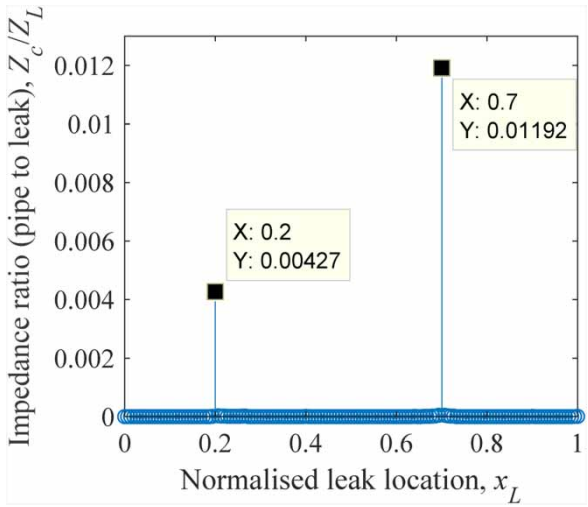


**Figure 6** | Results from the proposed leak detection technique showing the existence of two leaks (indicated by the two spikes), their normalized locations, and the corresponding values of impedance ratio (pipe to leak).

Note that if there is no leak, the result of $\mathrm{Im}\{U_{22} - U_{11}\}$ should be zero across all the frequencies.

### Leak detection

Leak detection is conducted by analyzing the numerically obtained $\mathrm{Im}\{U_{22} - U_{11}\}$ using the technique outline in Equations (25) and (26), and the results are shown in Figure 6. The two distinctive spikes indicate that there are two leaks in the pipe section of interest. The normalized locations are determined as $x_{L1} = 0.20$ and $x_{L2} = 0.70$, respectively, as shown by the $x$-axis, and the values of the impedance ratio are $Z_c/Z_{L1} = 0.00427$ and $Z_c/Z_{L2} = 0.0119$, respectively, according to the size of the two spikes. The results are highly consistent with the theoretical values as shown in Table 1. The successful detection has validated the effectiveness of the proposed targeted leak detection technique.

## Case 2: A pipe section in a pipe network

### System information

The layout of the pipeline system studied in Case 2 is given in Figure 7. The system is a simple pipe network with two reservoirs. Four pressure transducers are used ($T_A$ to $T_D$). The pipe section of interest is the section between $T_B$ and

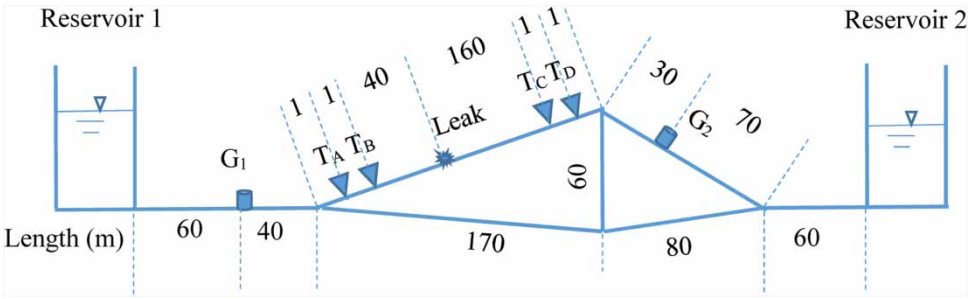


**Figure 7** | Layout of the simple pipe network in Case 2.

**Table 2** | System information for Case 2

| Parameter | Value |
|---|---|
| Head of reservoir 1, $H_{r1}$ | 60 m |
| Head of reservoir 2, $H_{r2}$ | 57 m |
| Internal diameter of all pipe sections, $D$ | 200 mm |
| Leak diameter, $D_L$ | 1.0 mm |
| Leak discharge coefficient, $C_d$ | 0.6 |
| Effective opening area of the leak, $C_dA_L$ | 0.47 mm$^2$ |
| Relative leak size, $C_dA_L/A$ | $1.5\times10^{-5}$ |
| Steady-state flow in the pipe directly downstream of the leak, $Q_0$ | 27.6 L/s |
| Steady-state flow through the leak, $Q_L$ | 0.016 L/s |
| Wave speed in all pipe sections, $a_0$ | 1000 m/s |
| Darcy–Weisbach friction factor, $f$ | 0.015 |
| Normalized location of the leak, $x_L$ | 0.2 |
| Impedance ratio of pipe to leak, $Z_c/Z_L$ | 4.4E–4 |

$T_C$, and one leak exists in this section. Two transient wave generators are used, which are placed on an upstream pipe section and a downstream pipe section, respectively. Key pipe system information is summarized in Table 2. The diameter of the leak is $D_L = 1.0$ mm, and the relative leak size is $1.5\times10^{-5}$ (0.015‰). This case represents a pin-hole leak on a water distribution pipe.

## Pressure response

The MOC (Wylie & Streeter 1993; Chaudhry 2014) is used to simulate the transient response of the simple pipe network system. Steady friction is considered to evaluate its impact on the leak detection. The time step used is 0.0002 s. Two transient tests are simulated using the generator $G_1$ and

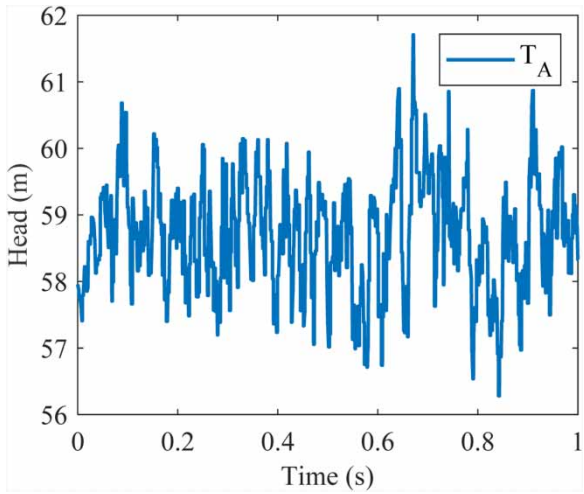


**Figure 8** | Pressure responses at $T_A$ as obtained from transient test 1 (using generator G1) in Case 2.

$G_2$, respectively. Considering the complexity of the network, the excitation signal used in both tests is a special type of pseudo-random binary signal (PRBS) – the inverse repeat signal (IRS) instead of discrete pulse or step signals. The IRS is a periodic signal that is suitable for extracting the pipeline frequency response (Gong *et al.* 2013a), and it can be generated by continuously altering the opening area of a side-discharge valve between two levels (Gong *et al.* 2016a). The IRS signal used in this study is the same as that described in Gong *et al.* (2013a) (simulating 10 shift registers with a clock frequency of 100 Hz) and has a period of 20.46 s. Each numerical test has a simulated time duration of 20 min, which is over 58 periods of the IRS. Spectrum analysis confirms that the pipe system reaches the steady oscillatory condition after 200 s (about 10 periods). A section of the pressure traces at $T_A$ as obtained from the first test is shown in Figure 8. Due to the pseudo-random

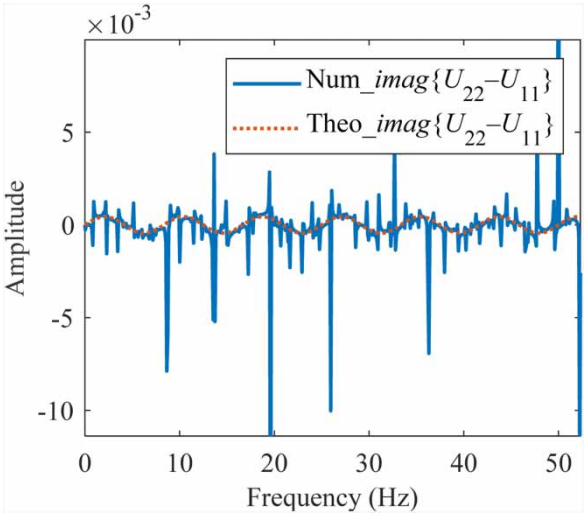


**Figure 9** | Imaginary part of ($U_{22} - U_{11}$) as obtained from numerical simulations and the proposed transfer matrix extraction technique for the pipe section with one leak in Case 2 (solid line), and the theoretical result for the same pipe section with one leak (dotted line).

nature of the excitation signal, the pressure response of the pipe system is complex and difficult to analyze directly in the time domain.

### Transfer matrix extraction

The same technique as outlined in previous sections can be used to extract the transfer matrix of the target pipe section.

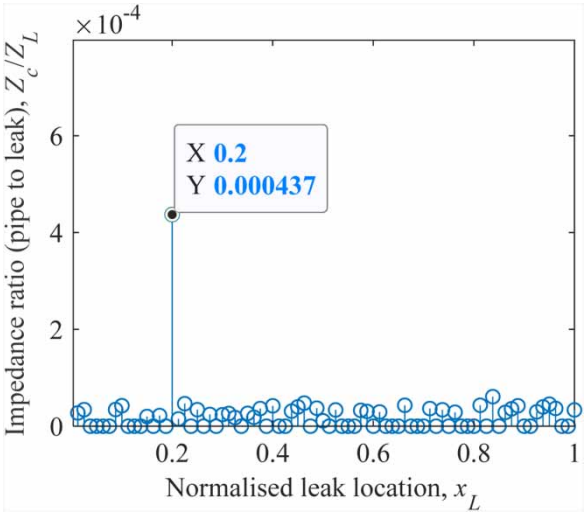


**Figure 10** | Leak detection results for Case 2 (1 mm leak) showing the existence of one leak (indicated by the single spike), the normalized leak location (0.2), and the corresponding impedance ratio (pipe to leak).

Since the excitation is a periodic signal, the pressure response should also be periodic once the pipe system is in the steady oscillatory condition (Wylie & Streeter 1993; Chaudhry 2014). The analysis in this numerical study only focuses on one period of the steady oscillatory pressure response for each sensor in each test. Averaging of the results from multiple periods may be needed in real applications. The determined $\mathrm{Im}\{U_{22} - U_{11}\}$ is shown in Figure 9, together with the theoretical result for comparison [using Equation (19)]. It can be seen that the numerically determined result has shown the expected sinusoidal pattern, despite the fact that there are a number of outliers due to the small size of the leak and the associated numerical uncertainties (caused by small denominators).

### Leak detection

Leak detection is conducted by analyzing the numerically obtained $\mathrm{Im}\{U_{22} - U_{11}\}$ using the technique outline in Equations (25) and (26), and the results are shown in Figure 10. The outliers, shown as the spikes in Figure 9, can be suppressed using signal processing techniques before the implementation of the Fourier transform for sinusoidal pattern extraction. In this research, hard thresholds and the Hampel filters (Liu *et al.* 2004) are used to suppress the outliers. The distinctive spike in Figure 10 indicates that there is one leak in the pipe section of interest. The normalized locations are determined as $x_L = 0.20$ from the $x$-axis, and the value of the impedance ratio is $Z_c/Z_L = 4.37 \times 10^{-4}$ according to the size of the spike. The results are highly consistent with the theoretical values as shown in Table 2. The successful detection has once again validated the effectiveness of the proposed targeted leak detection technique.

## DISCUSSION

### Sensitivity to leak size and measurement noise

Case study 2 has shown that pin-hole leaks as small as 1 mm in diameter can be successfully detected in a network environment using the proposed technique, provided that the pressure measurements are of high accuracy. Numerical uncertainties are observed in the analysis (Figure 9), and

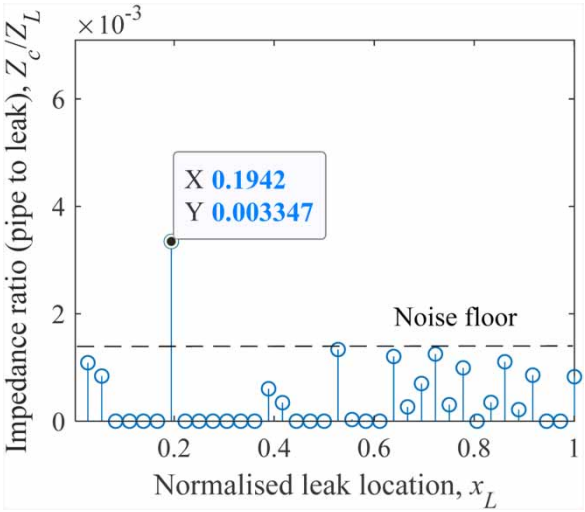


**Figure 11** | Leak detection results for the same system as Case 2 but with a 3 mm leak and measurement noise.

extra numerical simulations on larger leaks (not presented due to length limit) have demonstrated that the impact of the numerical uncertainty decreases with the increase of the leak size. Nevertheless, the impact of the numerical uncertainty is very limited and does not impede the accurate determination of the leak location and impedance.

Measurement noise can be an issue in application to real pipeline systems. The proposed technique uses wideband excitations (e.g. PRBS) and analyzes the corresponding wideband frequency responses. As a result, the analysis is expected to be tolerating to network background transient interference. Network background transient variations are mainly in the low frequency range (<20 Hz) and can be suppressed using high-pass filters (Gong *et al.* 2018b). They will not have much impact on the sinusoidal pattern in the higher frequencies.

Wideband noise, such as measurement uncertainties associated with the transducers or data acquisition systems, can potentially have a much more significant impact. To investigate the sensitivity, white noise with a standard deviation of 0.0033 m has been added to the pressure measurements in Case 2. This imposes a measurement uncertainty of ±0.01 m. Numerical simulations show that the 1 mm leak cannot be confidently detected with the presence of the noise. By incrementally increasing the leak size by 1 mm a step, the smallest leak that can be detected is found to be 3 mm ($C_d A_L/A = 1.35 \times 10^{-4}$, $Z_c/Z_L = 0.004$), as shown in Figure 11. More advanced signal processing may help to enhance the confidence of analysis and will be a topic of future research.

## Effect of friction

Friction is neglected in the proposed leak detection algorithm. The effect of friction on the frequency response of pipeline systems is minor and approximately uniform across all the frequencies (Lee *et al.* 2005); therefore, it should not affect the period of the sinusoidal waves in the $T_N$ signal or the localization of the leak. The impact of steady friction on the amplitude of the sinusoidal waves is very limited for real water transmission pipelines; therefore, the impact on the leak impedance/size determination is limited. The above has been confirmed by the two numerical case studies conducted in the current research, in which the locations of the leaks are accurately determined despite the fact that steady friction is included in the numerical simulations.

The unsteady friction, however, will induce a non-uniform dampening for the frequency responses, and a correction technique has been proposed in Lee *et al.* (2006). Recent research on the unsteady friction in water pipelines concludes that the effect of unsteady friction in large diameter water transmission pipelines is limited (Duan *et al.* 2011b; Vardy *et al.* 2015), and it has been generally neglected in practice (Shucksmith *et al.* 2012; Meniconi *et al.* 2013; Stephens *et al.* 2013). If the pipe section of interest (the section in bracket of the two pairs of transducers) is relatively long such that the fundamental frequency is low, the excitation and the analysis only need to focus on the low frequencies (e.g. in Case 1, the periodic nature of $\mathrm{Im}\{U_{22} - U_{11}\}$ is already clear in the range of 0–30 Hz; Fig. 6). In the low frequency range, the effect of unsteady friction is limited and less non-uniform.

## Other challenges in field application

Challenges are expected in real application of the proposed leak detection technique. Although the two-source-four-sensor testing configuration for water pipe transfer matrix extraction has been validated in the laboratory (Yamamoto *et al.* 2015), the implementation of this testing configuration in real pipe systems can be difficult. Transient generators (source) can be installed on existing access points such as

fire hydrants or air valves. The transducers need to be installed in pairs, and the distance between the two sensors in a pair needs to be short to enable the analysis. This is challenging since in real water pipelines it is uncommon to have two accessible points in close proximity. Recent research on fiber optic pressure sensor arrays (Gong *et al.* 2018c) may provide a solution in the future. It is envisaged that a fiber optic pressure sensor array, such as in the form of a flexible cable, can be inserted into a pipeline through a single access point. The same access point can also be used for transient wave generation. The fiber optic pressure sensors measure the transient response of the pipe system. The same configuration can be repeated at another access point to achieve the two-source-four-sensor testing configuration. Preliminary success has been achieved in the laboratory (Gong *et al.* 2018c); however, several design challenges need to be resolved to enhance the accuracy and robustness of the measurements.

The structural complexity of ageing pipelines can be another challenge. The proposed technique is a significant step forward to tackle complex pipe systems, and it enables a targeted pipe section to be visually isolated for independent analysis in any complex network. However, within the targeted pipe section, the condition of the pipe can still be complex, with the presence of not only leaks but non-uniform pipe wall deterioration. Duan *et al.* (2011a) demonstrated that FRF-based leak detection is applicable to complex series pipelines. Further research is needed to investigate the impact of pipe wall deterioration or other defects (e.g. blockages) in the targeted pipe section on leak detection.

## CONCLUSIONS

A new pipeline leak detection technique has been proposed in this research. The technique enables leak detection for a targeted pipe section independent of the complexities of the pipe system where the targeted section is embedded in. This is achieved by extracting the transfer matrix of the targeted pipe section using a two-source-four-sensor hydraulic transient testing strategy and analyzing the resultant transfer matrix by a newly developed algorithm. The proposed technique has been validated by two numerical case studies.

This research is a significant step toward the application of hydraulic transient-based leak detection techniques in real WDSs. The concept of virtually isolating a target pipe section out of a complex pipe system for independent analysis is useful not only for leak detection but also for other applications such as blockage detection and pipe wall condition assessment. Practical challenges, however, are expected in the field, and they include the implementation of the two-source-four-sensor testing configuration in buried pipelines and the structural uncertainties and complexities within the targeted pipe section. Further research, in particular experimental studies, is needed to solve these practical issues and enable a cost-effective application in the field.

## ACKNOWLEDGEMENTS

The research presented has been supported by the Australia Research Council through the Discovery Project Grant DP170103715 and DP190102484.

## REFERENCES

Beuken, R. H. S., Lavooij, C. S. W., Bosch, A. & Schaap, P. G. 2006 Low leakage in the Netherlands confirmed. In *Proceedings of the Water Distribution Systems Analysis Symposium 2006*. American Society of Civil Engineers, Reston, VA. doi:10.1061/40941(247)174.

Brunone, B., Ferrante, M. & Meniconi, S. 2008 Portable pressure wave-maker for leak detection and pipe system characterization. *Journal of American Water Works Association* **100** (4), 108–116. doi:10.1002/j.1551-8833.2008.tb09607.x.

Brunone, B., Meniconi, S. & Capponi, C. 2018 Numerical analysis of the transient pressure damping in a single polymeric pipe with a leak. *Urban Water Journal* **15** (8), 760–768. doi:10.1080/1573062X.2018.1547772.

Butterfield, J. D., Collins, R. P. & Beck, S. B. M. 2018 Influence of pipe material on the transmission of vibroacoustic leak signals in real complex water distribution systems: case study. *Journal of Pipeline Systems Engineering and Practice* **9** (3), 05018003. doi:10.1061/(ASCE)PS.1949-1204.0000321.

Capponi, C., Ferrante, M., Zecchin, A. C. & Gong, J. 2017 Leak detection in a branched system by inverse transient analysis with the admittance matrix method. *Water Resources Management* **31** (13), 4075–4089. doi:10.1007/s11269-017-1730-6.

Chaudhry, M. H. 2014 *Applied Hydraulic Transients*, 3rd edn. Springer, New York, NY.

Covas, D., Ramos, H. & De Almeida, A. B. 2005 Standing wave difference method for leak detection in pipeline systems. *Journal of Hydraulic Engineering* **131** (12), 1106–1116. doi:10.1061/(ASCE)0733-9429(2005)131:12(1106).

Cugueró-Escofet, M. À., Quevedo, J., Alippi, C., Roveri, M., Puig, V., García, D. & Trovò, F. 2016 Model- vs. data-based approaches applied to fault diagnosis in potable water supply networks. *Journal of Hydroinformatics* **18** (5), 831–850. doi:10.2166/hydro.2016.218.

Duan, H.-F. 2016 Transient frequency response based leak detection in water supply pipeline systems with branched and looped junctions. *Journal of Hydroinformatics* **19** (1), 17. doi:10.2166/hydro.2016.008.

Duan, H.-F., Lee, P. J., Ghidaoui, M. S. & Tung, Y.-K. 2011a Leak detection in complex series pipelines by using the system frequency response method. *Journal of Hydraulic Research* **49** (2), 213–221. doi:10.1080/00221686.2011.553486.

Duan, H.-F., Ghidaoui, M. S., Lee, P. J. & Tung, Y. K. 2011b Relevance of unsteady friction to pipe size and length in pipe fluid transients. *Journal of Hydraulic Engineering* **138** (2), 154–166. doi:10.1061/(asce)hy.1943-7900.0000497.

Ghazali, M. F., Beck, S. B. M., Shucksmith, J. D., Boxall, J. B. & Staszewski, W. J. 2012 Comparative study of instantaneous frequency based methods for leak detection in pipeline networks. *Mechanical Systems and Signal Processing* **29**, 187–200. doi:10.1016/j.ymssp.2011.10.011.

Gong, J., Simpson, A. R., Lambert, M. F. & Zecchin, A. C. 2013a Determination of the linear frequency response of single pipelines using persistent transient excitation: a numerical investigation. *Journal of Hydraulic Research* **51** (6), 728–734. doi:10.1080/00221686.2013.818582.

Gong, J., Lambert, M. F., Simpson, A. R. & Zecchin, A. C. 2013b Single-event leak detection in pipeline using first three resonant responses. *Journal of Hydraulic Engineering* **139** (6), 645–655. doi:10.1061/(ASCE)HY.1943-7900.0000720.

Gong, J., Stephens, M. L., Arbon, N. S., Zecchin, A. C., Lambert, M. F. & Simpson, A. R. 2015 On-site non-invasive condition assessment for cement mortar-lined metallic pipelines by time-domain fluid transient analysis. *Structural Health Monitoring* **14** (5), 426–438. doi:10.1177/1475921715591875.

Gong, J., Lambert, M. F., Zecchin, A. C. & Simpson, A. R. 2016a Experimental verification of pipeline frequency response extraction and leak detection using the inverse repeat signal. *Journal of Hydraulic Research* **54** (2), 210–219. doi:10.1080/00221686.2015.1116115.

Gong, J., Lambert, M. F., Zecchin, A. C., Simpson, A. R., Arbon, N. S. & Kim, Y.-I. 2016b Field study on non-invasive and non-destructive condition assessment for asbestos cement pipelines by time-domain fluid transient analysis. *Structural Health Monitoring* **15** (1), 113–124. doi:10.1177/1475921715624505.

Gong, J., Lambert, M. F., Nguyen, S. T. N., Zecchin, A. C. & Simpson, A. R. 2018a Detecting thinner-walled pipe sections using a spark transient pressure wave generator. *Journal of Hydraulic Engineering* **144** (2), 06017027. doi:10.1061/(ASCE)HY.1943-7900.0001409.

Gong, J., Nguyen, S. T. N., Stephens, M. L., Lambert, M. F., Marchi, A., Simpson, A. R. & Zecchin, A. C. 2018b Correlation of post-burst hydraulic transient noise for pipe burst/leak localisation in water distributions systems. In: *Proceedings of the 13th International Conference on Pressure Surges*. BHR Group, Cranfield, UK,

Gong, J., Png, G. M., Arkwright, J. W., Papageorgiou, A. W., Cook, P. R., Lambert, M. F., Simpson, A. R. & Zecchin, A. C. 2018c In-pipe fibre optic pressure sensor array for hydraulic transient measurement with application to leak detection. *Measurement* **126**, 309–317. doi:10.1016/j.measurement.2018.05.072.

Lee, P. J., Vítkovský, J. P., Lambert, M. F., Simpson, A. R. & Liggett, J. A. 2005 Leak location using the pattern of the frequency response diagram in pipelines: a numerical study. *Journal of Sound and Vibration* **284** (3–5), 1051–1073. doi:10.1016/j.jsv.2004.07.023.

Lee, P. J., Lambert, M. F., Simpson, A. R., Vítkovský, J. P. & Liggett, J. A. 2006 Experimental verification of the frequency response method for pipeline leak detection. *Journal of Hydraulic Research* **44** (5), 693–707. doi:10.1080/00221686.2006.9521718.

Li, R., Huang, H., Xin, K. & Tao, T. 2015 A review of methods for burst/leakage detection and location in water distribution systems. *Water Science and Technology* **15** (3), 429–441. doi:10.2166/ws.2014.131.

Liu, H., Shah, S. & Jiang, W. 2004 On-line outlier detection and data cleaning. *Computers & Chemical Engineering* **28** (9), 1635–1647. doi:10.1016/j.compchemeng.2004.01.009.

Meniconi, S., Brunone, B., Ferrante, M. & Massari, C. 2011 Potential of transient tests to diagnose real supply pipe systems: what can be done with a single extemporary test. *Journal of Water Resources Planning and Management* **137** (2), 238–241. doi:10.1061/(asce)wr.1943-5452.0000098.

Meniconi, S., Duan, H. F., Lee, P. J., Brunone, B., Ghidaoui, M. S. & Ferrante, M. 2013 Experimental investigation of coupled frequency and time-domain transient test-based techniques for partial blockage detection in pipelines. *Journal of Hydraulic Engineering* **139** (10), 1033–1044. doi:10.1061/(ASCE)HY.1943-7900.0000768.

Meniconi, S., Brunone, B., Ferrante, M., Capponi, C., Carrettini, C. A., Chiesa, C., Segalini, D. & Lanfranchi, E. A. 2015 Anomaly pre-localization in distribution–transmission mains by pump trip: preliminary field tests in the Milan pipe system. *Journal of Hydroinformatics* **17** (3), 377–389. doi:10.2166/hydro.2014.038.

Munjal, M. L. & Doige, A. G. 1990 Theory of a two source-location method for direct experimental evaluation of the four-pole parameters of an aeroacoustic element. *Journal of Sound and*

*Vibration* **141** (2), 323–333. doi:10.1016/0022-460X(90)90843-O.

Mutikanga, H. E., Sharma, S. & Vairavamoorthy, K. 2009 Water loss management in developing countries: challenges and prospects. *Journal of American Water Works Association* **101** (12), 57–68. doi:10.1002/j.1551-8833.2009.tb10010.x.

Nguyen, S. T. N., Gong, J., Lambert, M. F., Zecchin, A. C. & Simpson, A. R. 2018 Least squares deconvolution for leak detection with a pseudo random binary sequence excitation. *Mechanical Systems and Signal Processing* **99**, 846–858. doi:10.1016/j.ymssp.2017.07.003.

Oppenheim, A. V., Willsky, A. S. & Nawab, S. H. 1997 *Signals and Systems*, 2nd edn. Prentice Hall, Upper Saddle River, NJ.

Puust, R., Kapelan, Z., Savic, D. A. & Koppel, T. 2010 A review of methods for leakage management in pipe networks. *Urban Water Journal* **7** (1), 25–45. doi:10.1080/15730621003610878.

Salissou, Y. & Panneton, R. 2010 Wideband characterization of the complex wave number and characteristic impedance of sound absorbers. *The Journal of the Acoustical Society of America* **128** (5), 2868–2876. doi:10.1121/1.3488307.

Shi, H., Gong, J., Zecchin, A. C., Lambert, M. F. & Simpson, A. R. 2017 Hydraulic transient wave separation algorithm using a dual-sensor with applications to pipeline condition assessment. *Journal of Hydroinformatics* **19** (5), 752–765. doi:10.2166/hydro.2017.146.

Shi, H., Gong, J., Cook, P. R., Arkwright, J. W., Png, G. M., Lambert, M. F., Zecchin, A. C. & Simpson, A. R. 2019 Wave separation and pipeline condition assessment using in-pipe fibre optic pressure sensors. *Journal of Hydroinformatics* **21** (2), 371–379. doi:10.2166/hydro.2019.051.

Shucksmith, J. D., Boxall, J. B., Staszewski, W. J., Seth, A. & Beck, S. B. M. 2012 Onsite leak location in a pipe network by cepstrum analysis of pressure transients. *Journal of American Water Works Association* **104** (8), E457–E465. doi:10.5942/jawwa.2012.104.0108.

Soares, A. K., Covas, D. I. C. & Reis, L. F. R. 2010 Leak detection by inverse transient analysis in an experimental PVC pipe system. *Journal of Hydroinformatics* **13** (2), 153. doi:10.2166/hydro.2010.012.

Stephens, M. L., Lambert, M. F. & Simpson, A. R. 2013 Determining the internal wall condition of a water pipeline in the field using an inverse transient model. *Journal of Hydraulic Engineering* **139** (3), 310–324. doi:10.1061/(ASCE)HY.1943-7900.0000665.

Vardy, A. E., Brown, J. M. B., He, S., Ariyaratne, C. & Gorji, S. 2015 Applicability of frozen-viscosity models of unsteady wall shear stress. *Journal of Hydraulic Engineering* **141** (1), 04014064. doi:10.1061/(ASCE)HY.1943-7900.0000930.

Wang, X. J., Lambert, M. F., Simpson, A. R., Liggett, J. A. & Vítkovský, J. P. 2002 Leak detection in pipelines using the damping of fluid transients. *Journal of Hydraulic Engineering* **128** (7), 697–711. doi:10.1061/(ASCE)0733-9429(2002)128:7(697).

Wang, X., Lin, J., Keramat, A., Ghidaoui, M. S., Meniconi, S. & Brunone, B. 2019 Matched-field processing for leak localization in a viscoelastic pipe: an experimental study. *Mechanical Systems and Signal Processing* **124**, 459–478. doi:10.1016/j.ymssp.2019.02.004.

Wylie, E. B. & Streeter, V. L. 1993 *Fluid Transients in Systems*. Prentice Hall Inc., Englewood Cliffs, NJ, USA.

Yamamoto, K., Müller, A., Ashida, T., Yonezawa, K., Avellan, F. & Tsujimoto, Y. 2015 Experimental method for the evaluation of the dynamic transfer matrix using pressure transducers. *Journal of Hydraulic Research* **53** (4), 466–477. doi:10.1080/00221686.2015.1050076.

Zhang, C., Zecchin, A. C., Lambert, M. F., Gong, J. & Simpson, A. R. 2018 Multi-stage parameter-constraining inverse transient analysis for pipeline condition assessment. *Journal of Hydroinformatics* **20** (2). doi:10.2166/hydro.2018.154.

First received 5 October 2019; accepted in revised form 13 June 2020. Available online 16 July 2020